

# “Self-Wiener” Filtering: Non-Iterative Data-Driven Robust Deconvolution of Deterministic Signals

Amir Weiss and Boaz Nadler

**Abstract**—We consider the fundamental problem of robust deconvolution, and particularly the recovery of an unknown deterministic signal convolved with a known filter and corrupted by additive noise. We present a novel, non-iterative data-driven approach. Specifically, our algorithm works in the frequency-domain, where it tries to mimic the optimal unrealizable Wiener-like filter as if the unknown deterministic signal were known. This leads to a threshold-type regularized estimator, where the threshold value at each frequency is found in a fully data-driven manner. We provide an analytical performance analysis, and derive approximate closed-form expressions for the residual Mean Squared Error (MSE) of our proposed estimator in the low and high Signal-to-Noise Ratio (SNR) regimes. We show analytically that in the low SNR regime our method provides enhanced noise suppression, and in the high SNR regime it approaches the performance of the optimal unrealizable solution. Further, as we demonstrate in simulations, our solution is highly suitable for (approximately) bandlimited or frequency-domain sparse signals, and provides a significant gain of several dBs relative to other methods in the resulting MSE.

**Index Terms**—Deconvolution, system identification, Wiener filter.

## I. INTRODUCTION

A ubiquitous task in signal processing is *deconvolution* [1], namely inverting the action of some system (or channel) on an input, desired signal. A major difficulty arises when the measured convolved signal is contaminated with noise, wherein a careful balancing of bandwidth and Signal-to-Noise Ratio (SNR) is required [2]. This robust deconvolution problem appears in a wide variety of applications, such as communication systems, controllers, image and video processing, audio signal processing and ground-penetrating radar data analysis, to name but a few [3]–[9].

A common measure for the quality of the signal reconstructed from the noisy convolution measurements is the Mean Squared Error (MSE) between the unknown input signal and the deconvolved one. When the unknown signal and the noise are both modeled as stochastic stationary processes with known Second-Order Statistics (SOSs), the optimal solution within the class of linear estimators is the celebrated Wiener filter [10], [11]. Following Wiener’s work, many other deconvolution methods have been proposed, most of them under some *a-priori* knowledge about the class of the unknown input signals. For example, Berkhout [12] derived the least-squares inverse filtering for known noise SOSs, assuming that the input signal is white, namely with a constant spectral level. In [13], Eldar proposed a minimax approach, assuming the input signal

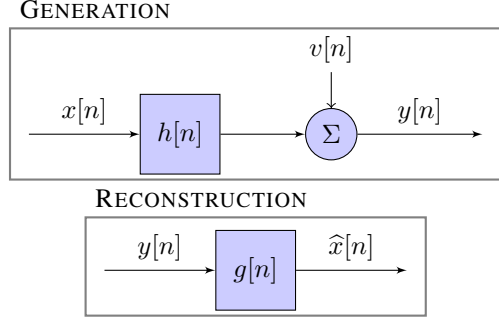


Fig. 1: Block diagram of model (1) (“GENERATION”), and the considered class of estimators, produced by filtering (“RECONSTRUCTION”). Note that in our framework,  $g[n]$  may depend on the measurements  $\{y[n]\}_{n=0}^{N-1}$ .

and noise are stochastic, with *a-priori* known upper and lower bounds on their spectra at each frequency.

While the random signal model is suitable in some problems and scenarios, in others the input signal is better modeled as *deterministic unknown*. Several methods have been proposed for this signal model as well [14]–[16]. One example is the WaveD algorithm proposed by Johnstone *et al.* [17], which is based on hard thresholding of a wavelet expansion (see also [18], Section II, for a concise description of WaveD). While some of these algorithms offer considerable enhancement, their performance may be affected by tuning parameters, which either need to be set by the user, or require separate careful calibration. Another class of deconvolution algorithms are iterative [19]–[23]. Some of these methods also require tuning parameters, such as the  $\lambda$  parameter in [19], controlling the balance between noise reduction and filtration errors, caused by the deviation from the ideal inverse filter when  $\lambda$  is non-zero. For a detailed discussion on this topic, see [24].

In this work, assuming known SOS of the noise, or an estimate thereof, we propose a novel non-iterative, computationally simple, *fully* data-driven deconvolution approach for deterministic signals. The guiding principle of our approach, termed “Self-Wiener” (SW) filtering, is an attempt to mimic the optimal Minimum MSE (MMSE) unrealizable Wiener-like filter, as if the unknown deterministic signal were known. This yields a self-consistent thresholding-type method with no tuning parameters. Our resulting threshold-type estimator is reminiscent of other thresholding methods (e.g., [25]), but due to its data-driven nature, it automatically computes a data-dependent threshold value. Moreover, this threshold can be intuitively explained from an estimated SNR perspective. We further present an analytical performance analysis of our proposed SW estimator, and derive approximate closed-form expressions for its predicted MSE. Comparison in simulations to other approaches, some of which are fully data-driven as

The authors are with the Department of Computer Science and Applied Mathematics, Faculty of Mathematics and Computer Science, Weizmann Institute of Science, 234 Herzl Street, Rehovot 7610001 Israel, e-mail: amir.weiss@weizmann.ac.il, boaz.nadler@weizmann.ac.il

well, show that our method offers highly competitive performance, and attains an MSE lower by several dBs for various signals representative of those appearing in applications.

## II. PROBLEM FORMULATION

Consider the classical discrete-time convolution model depicted in Fig. 1 (“GENERATION”),

$$y[n] = \sum_{k \in \mathbb{Z}} h[k]x[n-k] + v[n] \in \mathbb{R}, \quad \forall n \in \mathbb{Z}, \quad (1)$$

where  $h[n]$  is a known impulse response of a Linear Time-Invariant (LTI) system;  $x[n]$  is an unknown deterministic signal; and  $v[n]$  is a stationary, zero-mean additive noise with a positive Power Spectral Density (PSD) function, denoted by  $S_v(\omega)$ . We assume that the noise PSD  $S_v(\omega)$  is either known or has been estimated *a-priori*, e.g., from realizations of pure noise, measured in a “training period” [26]. We further assume that  $x[n]$  is periodic or has finite support, and that  $h[n]$  is a Finite Impulse Response (FIR) filter, which is compactly supported by definition, or at least may be well-approximated by an FIR filter.

The robust deconvolution problem [27] is to recover the signal  $x[n]$  based on the noisy measurements  $\{y[n]\}_{n=0}^{N-1}$ . Switching the roles of  $x[n]$  and  $h[n]$ , this problem is equivalent to the *system identification* problem [28]. In that context,  $x[n]$  is known and the problem is to estimate the unknown impulse response  $h[n]$ , namely to identify the system. Hence, while in this work we consider deconvolution, our proposed SW estimator is applicable to the system identification problem as well.

In the robust deconvolution context, the quality of an estimator  $\hat{x}[n]$  of  $x[n]$  is often measured by its MSE,

$$\text{MSE}(x, \hat{x}) \triangleq \mathbb{E} \left[ \sum_{n=0}^{N-1} |x[n] - \hat{x}[n]|^2 \right], \quad (2)$$

where the expectation is w.r.t. the noise  $v[n]$  in the observations  $y[n]$ , the only random component in the problem. In this work, we focus on deconvolution methods of the following form, as depicted in Fig. 1 (“RECONSTRUCTION”),

$$\hat{x}[n] = g[n] \otimes y[n], \quad \forall n \in \{0, \dots, N-1\}, \quad (3)$$

where  $\otimes$  denotes circular convolution. Hence the goal is to design a filter  $g[n]$  that gives a low MSE. In contrast to the classical linear Wiener filter, we allow the filter  $g[n]$  to depend on the observed signal  $y[n]$ , hence leading to a nonlinear estimator. To motivate our proposed filter, in Section III we first study the optimal unrealizable filter of the form (3), which depends on the unknown signal  $x[n]$ . Next, in Section IV we derive a realizable data-driven estimator that is close to the optimal unrealizable solution at low and high SNRs. As demonstrated in Section VI, our estimator achieves MSEs that can be several dB lower than other methods.

### A. Equivalent Formulation in the Frequency Domain

Due to our assumptions regarding the input signal  $x[n]$  and the FIR filter  $h[n]$ , given a finite number of samples

$\{y[n]\}_{n=0}^{N-1}$ , when  $N$  is sufficiently large, the linear convolution coincides or may be well-approximated by circular convolution (neglecting boundary effects) [29]. Hence, we consider the problem in the frequency domain.

Recall that the unitary Discrete Fourier Transform (DFT) of a length- $N$  sequence  $a[n]$  is defined as

$$A[k] \triangleq \text{DFT}\{a[n]\} \triangleq \frac{1}{\sqrt{N}} \sum_{n=0}^{N-1} a[n] e^{-j\frac{2\pi}{N}nk} \in \mathbb{C}, \quad (4)$$

for all  $k \in \{0, \dots, N-1\}$ . Since circular convolution in the discrete-time domain is equivalent to multiplication in the (discrete-)frequency domain, applying the DFT to the sequence  $\{y[n]\}_{n=0}^{N-1}$  (1) gives

$$Y[k] = H[k]X[k] + V[k] \in \mathbb{C}, \quad \forall k \in \{0, \dots, N-1\},$$

and (3) becomes  $\hat{X}[k] = G[k]Y[k]$ . Since the DFT is a unitary transformation, by Parseval’s identity

$$\text{MSE}(x, \hat{x}) = \sum_{k=0}^{N-1} \mathbb{E} \left[ |X[k] - \hat{X}[k]|^2 \right] \triangleq \sum_{k=0}^{N-1} \text{MSE}[k], \quad (5)$$

where, with a slight abuse in notation,

$$\text{MSE}[k] \triangleq \mathbb{E} \left[ |X[k] - \hat{X}[k]|^2 \right] = \mathbb{E} \left[ |X[k] - G[k]Y[k]|^2 \right] \quad (6)$$

denotes the MSE at the  $k$ -th frequency component. Obviously, *individually* minimizing each term  $\text{MSE}[k]$  in the sum (5), minimizes the MSE (2). However, when  $x[n]$ , or equivalently  $X[k]$ , is assumed deterministic, the resulting optimal solution— $\hat{X}_{\text{opt}}[k]$ , to be introduced shortly in (11) below—is not a realizable estimator, as we show next.

## III. THE OPTIMAL DECONVOLUTION MMSE SOLUTION

To motivate our proposed estimator, it is first instructive to present the structure of the optimal, yet not realizable solution, which minimizes (2) over all estimators of the form (3). For this, let us begin by introducing the following quantities:

$$\text{SNR}[k] \triangleq \frac{|X[k]|^2}{S_v[k]}, \quad \text{SNR}_{\text{out}}[k] \triangleq \frac{|H[k]X[k]|^2}{S_v[k]}, \quad (7)$$

where

$$S_v[k] \triangleq S_v(\omega) \Big|_{\omega=\frac{2\pi k}{N}} = S_v\left(\frac{2\pi k}{N}\right)$$

is the noise PSD at the  $k$ -th frequency. By definition,  $\text{SNR}[k]$  and  $\text{SNR}_{\text{out}}[k]$  are the SNRs at the  $k$ -th frequency of the noise-free signal  $x[n]$  and of its convolution with  $h[n]$ , at the output of the system, respectively. Since  $x[n]$  is unknown, both quantities are unknown. Further, we define

$$\hat{X}_{\text{LS}}[k] \triangleq \frac{Y[k]}{H[k]}, \quad \forall k \in \{0, \dots, N-1\}, \quad (8)$$

which is the naïve Least-Squares (LS) estimator of  $X[k]$ , obtained by filtering the noisy measurements using the inverse of the known filter  $H[k]$ , assuming  $H[k] \neq 0$ .

The optimal MMSE filter  $G_{\text{opt}}[k]$  may be found by differentiating (6) w.r.t.  $G^*[k]$  and equating to zero. This gives

$$-|X[k]|^2 H^*[k] + G[k] \mathbb{E} \left[ |X[k]H[k] + V[k]|^2 \right] = 0, \quad (9)$$

where we have used  $\mathbb{E}[V^*[k]] = 0$ . Since the noise  $v[n]$  is stationary, for a sufficiently large  $N$  (see e.g. [30]),

$$\mathbb{E}[|V[k]|^2] \underset{N \gg 1}{\approx} S_v[k].$$

Thus, after simplifying and arranging the terms in (9), the optimal deconvolving filter at the  $k$ -th frequency is

$$G_{\text{opt}}[k] \triangleq \frac{H^*[k]}{|H[k]|^2 + \frac{S_v[k]}{|X[k]|^2}} = \frac{H^*[k]}{|H[k]|^2 + \frac{1}{\text{SNR}[k]}}. \quad (10)$$

Accordingly, the corresponding optimal solution is given by

$$\widehat{X}_{\text{opt}}[k] = Y[k]G_{\text{opt}}[k] = \widehat{X}_{\text{LS}}[k] \cdot \frac{1}{1 + \frac{1}{\text{SNR}_{\text{out}}[k]}}. \quad (11)$$

The resulting MMSE at the  $k$ -th frequency in the class of estimators of the form (3) is thus

$$\begin{aligned} \text{MMSE}[k] &\triangleq \mathbb{E} \left[ |X[k] - \widehat{X}_{\text{opt}}[k]|^2 \right] \\ &= \frac{|X[k]|^2}{1 + \text{SNR}_{\text{out}}[k]} = \sigma_{\text{eff}}^2[k] \cdot \frac{1}{1 + \frac{1}{\text{SNR}_{\text{out}}[k]}}, \end{aligned} \quad (12)$$

where  $\sigma_{\text{eff}}^2[k]$  is the effective noise level at the system output  $k$ -th frequency, defined for all  $k \in \{0, \dots, N-1\}$  as

$$\sigma_{\text{eff}}^2[k] \triangleq \frac{S_v[k]}{|H[k]|^2}. \quad (13)$$

As seen from (10) and (7), the optimal deconvolution filter does not yield a realizable estimator, since it depends on  $\text{SNR}[k]$ , which in turn depends on the unknown signal  $x[n]$ . Accordingly, the MMSE (12) is equal to the effective noise level at the output of the system multiplied by a regularizing term, which also depends on the unknown signal  $x[n]$ . Further, observe that when  $|X[k]|^2 \rightarrow \infty$  while  $\sigma_{\text{eff}}^2[k]$  is fixed, and thus  $\text{SNR}_{\text{out}}[k] \rightarrow \infty$ , the MMSE (12) reads

$$\text{MMSE}[k] \xrightarrow[\sigma_{\text{eff}}^2 \text{ fixed}]{\text{SNR}_{\text{out}}[k] \rightarrow \infty} \sigma_{\text{eff}}^2[k].$$

Hence infinite output SNR does not guarantee perfect reconstruction at the output of the system even for the optimal unrealizable solution. However, when  $\sigma_{\text{eff}}^2[k] \rightarrow 0$  while  $X[k]$  is fixed, which also implies  $\text{SNR}_{\text{out}}[k] \rightarrow \infty$ , the MMSE (12) converges to zero, which corresponds to perfect reconstruction.

It is interesting to note the resemblance of  $G_{\text{opt}}[k]$  to the Wiener filter. Indeed, in case the input signal  $x[n]$  is a stationary stochastic process with a known PSD function, the Wiener filter has a form similar to (10), but with  $|X[k]|^2$  replaced by the PSD of  $x[n]$ .

#### IV. "SELF-WIENER" FILTERING

The structure of the optimal solution (11) motivates the following iterative approach: Start from an initial estimate of  $X[k]$ , and use it to estimate the quantity  $\text{SNR}_{\text{out}}[k]$  defined in (7). Then, plug this into (11) to obtain an improved estimate of  $X[k]$ . This principle leads to the following iterative procedure,

$$\widehat{X}_{\text{sw}}^{(t+1)}[k] = \widehat{X}_{\text{LS}}[k] \cdot \frac{1}{1 + \frac{\sigma_{\text{eff}}^2[k]}{|\widehat{X}_{\text{sw}}^{(t)}[k]|^2}}, \quad \forall t \in \mathbb{N}_0, \quad (14)$$

starting from some  $\widehat{X}_{\text{sw}}^{(0)}[k]$ . The following theorem shows that, when initialized with the LS estimator (8), these iterations converge to a limit with a simple explicit form. The result described in (16) below is our proposed estimator.

*Theorem 1: Let  $\widehat{X}_{\text{sw}}^{(0)}[k] = \widehat{X}_{\text{LS}}[k]$ . Then, at each frequency  $k$ , the iterations (14) converge to a solution  $\widehat{X}_{\text{sw}}[k]$ , which satisfies*

$$\widehat{X}_{\text{sw}}[k] = \widehat{X}_{\text{LS}}[k] \cdot \frac{1}{1 + \frac{\sigma_{\text{eff}}^2[k]}{|\widehat{X}_{\text{sw}}[k]|^2}}. \quad (15)$$

*The solution of (15) is the following thresholding operator*

$$\widehat{X}_{\text{sw}}[k] \triangleq \widehat{X}_{\text{LS}}[k] \cdot \begin{cases} \frac{2|Z[k]|^{-2}}{1 - \sqrt{1 - 4|Z[k]|^{-2}}}, & |Z[k]| > 2 \\ 0, & |Z[k]| < 2 \end{cases}, \quad (16)$$

where

$$Z[k] \triangleq \frac{Y[k]}{\sqrt{S_v[k]}}, \quad \forall k \in \{0, \dots, N-1\}. \quad (17)$$

In the proof of Theorem 1, we use the following result from stability theory (e.g., [31]):

*Theorem 2: Let  $\gamma_*$  be a fixed point of a continuously differentiable function  $f : \mathbb{R} \rightarrow \mathbb{R}$ . Then  $\gamma_*$  is stable if  $|f'(\gamma_*)| < 1$ , and unstable if  $|f'(\gamma_*)| > 1$ .*

*Proof of Theorem 1:* First, notice that the phase of the estimator (14) remains constant throughout the iterative process. Further, note that the phase of the optimal MMSE solution (11) is equal to the phase of the LS estimator (8). Hence, we focus on the convergence of the proposed estimator's magnitude. Furthermore, for ease of notation, let us define the following three quantities, omitting  $k$  for brevity:  $\gamma_t \triangleq \frac{1}{|\widehat{X}_{\text{sw}}^{(t)}[k]|}$ , the reciprocal magnitude of  $\widehat{X}_{\text{sw}}^{(t)}[k]$ , and  $\alpha \triangleq \frac{1}{|\widehat{X}_{\text{LS}}[k]|}$ ,  $\beta^2 \triangleq \sigma_{\text{eff}}^2[k]$ , which are constants throughout the iterative process, independent of the iteration index,  $t$ . With these notations, the iterations (14) take the form

$$\gamma_{t+1} = \alpha \cdot (1 + \beta^2 \cdot \gamma_t^2) \triangleq f(\gamma_t) \in \mathbb{R}^+, \quad \forall t \in \mathbb{N}_0. \quad (18)$$

Note that convergence of  $\gamma_t$  is equivalent to convergence of  $|\widehat{X}_{\text{sw}}^{(t)}[k]|$ . The convergence of this recursive formula may be analyzed using principles from stability theory. First, notice that due to the randomness of  $\alpha$ , the quadratic equation  $f(\gamma) = \gamma$  has either two solutions or none almost surely (i.e., it has one solution with zero probability). Thus, when  $\alpha^2\beta^2 > 1/4$ , there is no fixed point, and since  $\gamma_t \geq 0$ , it follows that  $f'(\gamma_t) > 0$  for all  $t \in \mathbb{N}_0$ , and  $\gamma_t$  diverges. When  $\alpha^2\beta^2 < 1/4$ , there are two fixed points, with only one of them stable. Applying Theorem 2 to our transformed iterative procedure (18), one easily obtains that starting with  $\gamma_0 = \alpha$ ,

$$\gamma_t \xrightarrow[t \rightarrow \infty]{} \begin{cases} \frac{1 - \sqrt{1 - 4\alpha^2\beta^2}}{2\alpha\beta^2} \triangleq \gamma_*, & \alpha^2\beta^2 < 1/4 \\ \infty, & \alpha^2\beta^2 > 1/4 \end{cases}. \quad (19)$$

Finally, since  $(\alpha\beta)^{-2} = |Z[k]|^2$ , inverting (19) and multiplying by  $\widehat{X}_{\text{LS}}[k]/|\widehat{X}_{\text{LS}}[k]|$  yields (16). ■

Note that since  $f(\gamma)$  is quadratic, when  $\alpha^2\beta^2 < 1/4$ , the iterative process in fact converges to  $\gamma_*$  from any initial

value  $\gamma_0 \in [0, \gamma_*]$ . Specifically, with  $\gamma_0 = 0$ , rather than  $\gamma_0 = \alpha$  as suggested in the theorem, we again obtain  $\gamma_1 = \alpha$ , corresponding to the initial solution  $\widehat{X}_{\text{sw}}^{(1)}[k] = \widehat{X}_{\text{LS}}[k]$ .

An equivalent, yet different enlightening expression for the SW estimator (16) is given as follows. Focusing on the case  $|Z[k]| > 2$ , by multiplying the numerator and denominator in (16) by  $1 + \sqrt{1 - 4|Z[k]|^{-2}}$ , we obtain

$$\widehat{X}_{\text{sw}}[k] = \widehat{X}_{\text{LS}}[k] \cdot \frac{1}{2} \left( 1 + \sqrt{1 - 4|Z[k]|^{-2}} \right). \quad (20)$$

The form (20) illustrates the *shrinkage* of the SW filter w.r.t. the naïve LS estimator, with the shrinkage factor depending on the observed value  $Z[k]$ . At a high output SNR,  $|Z[k]| \gg 1$  with high probability, and there is almost no shrinkage. In contrast, if  $|Z[k]| \rightarrow 2$  from above, the shrinkage tends to  $1/2$ . In the complementary case  $|Z[k]| < 2$ , the shrinkage factor is strictly zero. This can be interpreted as if the SW estimator “prefers” in this case an effective noise suppression at the cost of (potential) poor estimation accuracy. Interestingly, this behavior of the proposed SW estimator is reminiscent of thresholding methods in high dimensional statistics, in particular in the presence of sparsity (e.g., [32]). We thus expect our estimator to be superior to other, non-threshold-type estimators for signals with low energy in certain frequency components, such as bandlimited or sparse frequency-domain signals (e.g., [33], [34]). This will be illustrated via simulations in Section VI.

We now provide some intuition for our proposed estimator, (16). Note that the unrealizable optimal solution (11) is the LS estimator multiplied by a regularization term, which depends on the unknown  $X[k]$ . Similarly, the proposed estimator, which is the solution of (15), is also the LS estimator multiplied by a regularization term with the same structure as the optimal one. However, since  $X[k]$  is unknown, our self-consistent estimator “uses itself” to construct the regularization term. Hence the name of the proposed method—“Self-Wiener” filtering. This intuition can be rigorously justified in the high SNR regime, as shown next.

#### A. The Self-Wiener Estimator in the High SNR Regime

Let us present another interpretation which sheds light from a different angle on the successful mode of operation of our proposed estimator (16). Specifically, we now show that our estimator approximately coincides with the optimal solution (11) in the high SNR regime.

Recall that since  $Y[k] = H[k]X[k] + V[k]$ , then

$$Z[k] = \frac{H[k]X[k]}{\sqrt{S_v[k]}} + \frac{V[k]}{\sqrt{S_v[k]}} \triangleq \eta[k] + \widetilde{V}[k]. \quad (21)$$

Hence  $\text{SNR}_{\text{out}}[k] = |\eta[k]|^2$ , which naturally leads to the definition

$$\widehat{\text{SNR}}_{\text{out}}[k] \triangleq |Z[k]|^2 = |\eta[k] + \widetilde{V}[k]|^2. \quad (22)$$

At a high output SNR, where  $|\eta[k]| \gg 1$ , with high probability  $|Z[k]| \gg 2$ , and thus  $4|Z[k]|^{-2} \ll 1$ . Using the second-order Taylor expansion  $\sqrt{1 - x} \approx 1 - \frac{x}{2} - \frac{x^2}{8}$  (valid for any  $|x| \ll 1$ ),

$$\frac{2|Z[k]|^{-2}}{1 - \sqrt{1 - 4|Z[k]|^{-2}}} \approx \frac{1}{1 + |Z[k]|^{-2}}. \quad (23)$$

Combining (22) and (23) yields that at  $\text{SNR}_{\text{out}}[k] \gg 1$ ,

$$\widehat{X}_{\text{sw}}[k] \approx \widehat{X}_{\text{LS}}[k] \cdot \frac{1}{1 + \frac{1}{\widehat{\text{SNR}}_{\text{out}}[k]}}. \quad (24)$$

Evidently, (24) has the same structure as the optimal solution (11), but uses the estimated output SNR rather than the true output SNR. Hence, our proposed estimator is a nearly optimal fully data-driven approximation of (11) when  $X[k]$  is unknown.

Note further that, in the case where the noise spectrum  $S_v[k]$  is not known *a-priori*, (16) may also be computed with an estimated noise spectrum, denoted by  $\widehat{S}_v[k]$ , replacing  $S_v[k]$ . That is, given an estimator  $\widehat{S}_v[k]$ , which may be obtained by pre-access to a noise (only) realization or directly from the measured noisy convoluted data (e.g., as in [35], Subsection 6.1.1, for white noise), we define  $\widehat{Z}[k] \triangleq Y[k]/\sqrt{\widehat{S}_v[k]}$ , and replace  $Z[k]$  with  $\widehat{Z}[k]$  everywhere in (16).

We now turn to a statistical performance analysis of the proposed estimator, which allows to accurately assess its performance in terms of its MSE.

#### V. MSE ANALYSIS OF THE PROPOSED ESTIMATOR

In this section we derive closed-form approximate expressions for the MSE of our proposed SW estimator (16). Since our estimator operates in the frequency domain, using (5) we may write

$$\text{MSE}(x, \widehat{x}_{\text{sw}}) = \sum_{k=0}^{N-1} \mathbb{E} \left[ \left| X[k] - \widehat{X}_{\text{sw}}[k] \right|^2 \right] \triangleq \sum_{k=0}^{N-1} \text{MSE}_{\text{sw}}[k],$$

where the expectation is over the random noise  $V[k]$ , a function of  $\{v[n]\}_{n=0}^{N-1}$  of (1). Further, recall that the signal  $x[n]$  is considered deterministic, and is therefore fixed w.r.t. the expectation. We also define  $p[k] \triangleq \Pr(|Z[k]| > 2)$ , which is the probability that  $|Z[k]|$  from (17) will be above the threshold, according to (16). Thus, we shall focus on the MSE at the  $k$ -th frequency component,  $\text{MSE}_{\text{sw}}[k]$ . Using (16) and invoking the law of total expectation, we have

$$\begin{aligned} \text{MSE}_{\text{sw}}[k] &= p[k] \cdot \mathbb{E} \left[ \left| X[k] - \widehat{X}_{\text{sw}}[k] \right|^2 \middle| |Z[k]| > 2 \right] + \\ &\quad (1 - p[k]) \cdot \mathbb{E} \left[ \left| X[k] - \underbrace{\widehat{X}_{\text{sw}}[k]}_{=0} \right|^2 \middle| |Z[k]| \leq 2 \right]. \end{aligned} \quad (25)$$

Inserting the following relation

$$\left| X[k] - \widehat{X}_{\text{sw}}[k] \right|^2 = |X[k]|^2 + \left| \widehat{X}_{\text{sw}}[k] \right|^2 - 2\Re \left\{ \widehat{X}_{\text{sw}}[k] X^*[k] \right\}$$

into (25), we obtain after simplification

$$\begin{aligned} \text{MSE}_{\text{sw}}[k] &= |X[k]|^2 + p[k] \cdot \mathbb{E} \left[ \left| \widehat{X}_{\text{sw}}[k] \right|^2 \middle| |Z[k]| > 2 \right] \\ &\quad - 2p[k] \cdot \Re \left\{ X^*[k] \cdot \mathbb{E} \left[ \widehat{X}_{\text{sw}}[k] \middle| |Z[k]| > 2 \right] \right\}. \end{aligned} \quad (26)$$

From this point on, we assume that the noise  $V[k]$  is a Complex Normal (CN) Random Variable (RV). Thus, it follows that  $Z[k] \sim \mathcal{CN}(\eta[k], 1)$ , where  $\eta[k]$  is defined in (21). Indeed, this holds when the time-domain additive noise  $v[n]$



is Gaussian. Nonetheless, as seen from the DFT definition (4), for a sufficiently large  $N$  this is also approximately true (under mild conditions) due to the Central Limit Theorem (CLT) [36]. In addition, for the sake of brevity, throughout this section we omit the frequency index  $k$  hereafter. However, we emphasize that the following analysis is *per frequency*, and the overall performance depends on the sum of all the MSEs at all frequencies. Additionally, here we analyze only the complex-valued frequency bins, corresponding to all the indices except for  $k = 0, N/2$ . The later, which correspond to real-valued DFT components, are addressed in Appendix C (in a similar manner).

In order to obtain general closed-form expressions of the MSE (26), one must compute the conditional expectations

$$\mathbb{E} \left[ \widehat{X}_{\text{sw}} \middle| |Z| > 2 \right] = \frac{\sqrt{S_v}}{H} \mathbb{E} \left[ \frac{2(Z^*)^{-1}}{1 - \sqrt{1 - 4|Z|^{-2}}} \middle| |Z| > 2 \right], \quad (27)$$

$$\mathbb{E} \left[ \left| \widehat{X}_{\text{sw}} \right|^2 \middle| |Z| > 2 \right] = \frac{S_v}{|H|^2} \mathbb{E} \left[ \frac{4|Z|^{-2}}{(1 - \sqrt{1 - 4|Z|^{-2}})^2} \middle| |Z| > 2 \right], \quad (28)$$

as well as an expression for the probability  $p$ . In the next subsections we derive relatively simple approximations to these expectations at both low and high SNR regimes, leading to insightful approximate expressions of the SW estimator's MSE (26). We begin with the derivation of the probability  $p$ .

Using the notations  $Z_r \triangleq \Re\{Z\}$  and  $Z_i \triangleq \Im\{Z\}$ , such that

$$Z_r \sim \mathcal{N}(\Re\{\eta\}, \frac{1}{2}), \quad Z_i \sim \mathcal{N}(\Im\{\eta\}, \frac{1}{2}),$$

we have

$$\begin{aligned} p &= \Pr(|Z| > 2) = \Pr(|Z|^2 > 4) \\ &= \Pr\left(\left(\sqrt{2}Z_r\right)^2 + \left(\sqrt{2}Z_i\right)^2 > 8\right) \triangleq \Pr(\Xi > 8), \end{aligned}$$

where  $\Xi$  is by definition a non-central chi-square RV with two degrees of freedom and a non-centrality parameter  $2|\eta|^2$ . Thus,

$$\begin{aligned} p &= \Pr(\Xi > 8) = Q_1(\sqrt{2} \cdot |\eta|, 2\sqrt{2}) \\ &= Q_1(\sqrt{2 \cdot \text{SNR}_{\text{out}}}, 2\sqrt{2}), \end{aligned} \quad (29)$$

where we have used  $\text{SNR}_{\text{out}} = |\eta|^2$ , and

$$Q_M(a, b) \triangleq \int_b^\infty x \left(\frac{x}{a}\right)^{M-1} e^{-\frac{x^2+a^2}{2}} I_{M-1}(ax) dx$$

is the Marcum Q-function [37], where  $I_{M-1}(\cdot)$  is the modified Bessel function of order  $M - 1$ . It is easy to verify that,

$$p = Q_1(\sqrt{2 \cdot \text{SNR}_{\text{out}}}, 2\sqrt{2}) \xrightarrow{\text{SNR}_{\text{out}} \rightarrow \infty} 1, \quad (30)$$

as illustrated in Fig. 2. Hence, at frequencies with high output SNR, (25) becomes

$$\text{MSE}_{\text{sw}} \xrightarrow{\text{SNR}_{\text{out}} \rightarrow \infty} \mathbb{E} \left[ \left| X - \widehat{X}_{\text{sw}} \right|^2 \middle| |Z| > 2 \right], \quad (31)$$

where  $\widehat{X}_{\text{sw}}$  in (31) is given by (24). Therefore, in compliance with the interpretation given in Subsection IV-A, the MSE of the SW estimator at high output SNR is nearly the MMSE (12) of the optimal solution (11), as expected.

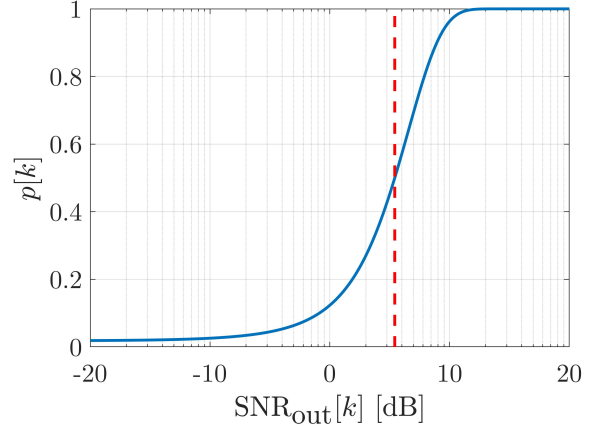


Fig. 2: Probability of the  $k$ -th frequency to be above the threshold vs. the output SNR (7). The dashed red line marks the point where  $p[k] = 0.5$ .

#### A. Approximate MSE at Frequencies with Low SNR

Recall that  $\text{SNR}_{\text{out}} = |\eta|^2$ , hence in the low SNR regime  $|\eta| \ll 1$ . Accordingly, we have the following theorem, whose proof appears in Appendix A.

*Theorem 3: At frequencies with low SNR, namely with  $|\eta| \ll 1$ , the MSE (26) is given by*

$$\begin{aligned} \text{MSE}_{\text{sw}} &= |X|^2 + \rho \cdot \sigma_{\text{eff}}^2 + \mathcal{O}(|\eta|) \\ &= |X|^2 \cdot \left(1 + \frac{\rho}{\text{SNR}_{\text{out}}}\right) + \mathcal{O}(\sqrt{\text{SNR}_{\text{out}}}) \triangleq \varepsilon_{\text{low}}^2, \end{aligned} \quad (32)$$

where the scalar  $\rho \approx 0.0464$  is defined explicitly in (51).

As a “sanity check”, notice that for frequencies containing only noise, namely  $X = 0$ , we have

$$\text{MSE}_{\text{sw}} = \rho \cdot \sigma_{\text{eff}}^2, \quad (33)$$

so the residual MSE of the SW estimator depends only on  $\sigma_{\text{eff}}^2$ , i.e., on the ratio  $S_v/|H|^2$ . As expected, if at some frequency  $H$  is very close to zero, noise amplification occurs, but with a considerable suppression due to  $\rho$ . For example, comparing the MSE (33) to the (unbiased) LS estimator's (8) MSE,

$$X = 0 : \text{MSE}_{\text{sw}} = \rho \cdot \sigma_{\text{eff}}^2 \ll \sigma_{\text{eff}}^2 = \text{MSE}_{\text{LS}}, \quad (34)$$

a reduction of more than an order of magnitude ( $\sim 13$ [dB]).

Nevertheless, this “defense mechanism” is of course limited due to the fact that  $X$  is unknown. Indeed, the SW estimator, as any other estimator in this setup, cannot accurately distinguish between the presence of a dominant signal and a highly “energized” realization of noise, which is manifested as a large estimated output SNR (22). Consequently, in the later case,  $|Z|$  will be above the threshold, causing an erroneous estimate.

One can now also quantify the *optimality gap* from the MSE (12) of the unrealizable MMSE solution (11) in the low SNR regime, which is given approximately by

$$\text{MSE}_{\text{sw}} - \text{MMSE} \approx |X|^2 \cdot \left( \frac{\text{SNR}_{\text{out}} + \rho(1 + \text{SNR}_{\text{out}}^{-1})}{1 + \text{SNR}_{\text{out}}} \right), \quad (35)$$

neglecting the  $\mathcal{O}(\sqrt{\text{SNR}_{\text{out}}})$  term. Although the SW estimator provides significant noise-suppression relative to the LS estimator (34), we see from (35) that when the output

SNR approaches zero, the optimality gap approaches infinity. This unfortunate outcome is also expected since the optimal unrealizable solution uses knowledge of the unknown signal itself in order to suppress noise at low SNRs. Obviously, this knowledge is not available for any realizable estimator.

### B. Approximate MSE at Frequencies with High SNR

In the high SNR regime  $|\eta| \gg 1$ , we have the following theorem, whose proof appears in Appendix B.

*Theorem 4: At frequencies with high SNR, namely with  $|\eta| \gg 1$ , the MSE (26) is given by*

$$\begin{aligned} \text{MSE}_{\text{sw}} &= (1-p) \cdot |X|^2 + p \cdot \frac{|X|^2}{|\eta|^2} + \mathcal{O}\left(\frac{|X|^2}{|\eta|^4}\right) \\ &= (1-p) \cdot |X|^2 + p \cdot \sigma_{\text{eff}}^2 + \mathcal{O}\left(\frac{\sigma_{\text{eff}}^2}{\text{SNR}_{\text{out}}}\right) \triangleq \varepsilon_{\text{high}}^2, \end{aligned} \quad (36)$$

where  $p = Q_1\left(\sqrt{2 \cdot \text{SNR}_{\text{out}}}, 2\sqrt{2}\right)$  as in (29).

In principle, from properties of Marcum Q-function, as  $|\eta| \rightarrow \infty$ ,  $p \rightarrow 1$  exponentially fast in  $|\eta|$ . When the output SNR is sufficiently high and  $p \approx 1$  as in (30), the optimality gap is approximately given by

$$\text{MSE}_{\text{sw}} - \text{MMSE} \approx \sigma_{\text{eff}}^2 \cdot \frac{1}{1 + \text{SNR}_{\text{out}}}. \quad (37)$$

Following the discussion in Subsection IV-A, (37) shows that the optimality gap approaches zero as the output SNR approaches infinity,

$$\text{MSE}_{\text{sw}} - \text{MMSE} \underset{\text{SNR}_{\text{out}} \gg 1}{\approx} \frac{\sigma_{\text{eff}}^2}{\text{SNR}_{\text{out}}} \xrightarrow{\text{SNR}_{\text{out}} \rightarrow \infty} 0. \quad (38)$$

We thus conclude that our proposed SW estimator converges to the optimal unrealizable solution as  $\text{SNR}_{\text{out}} \rightarrow \infty$ .

Having obtained approximated closed-form expressions for the MSE at low and high SNRs, for the intermediate SNR interval, we propose to interpolate between (32) and (36). Specifically, for some fixed value  $\tau \in \mathbb{R}^+$ , we define

$$f_{\tau}(\text{SNR}_{\text{out}}) \triangleq \frac{1}{2} \cdot \left(1 - \frac{\text{SNR}_{\text{out}}[\text{dB}]}{\tau[\text{dB}]}\right), \quad \forall \text{SNR}_{\text{out}} \in [-\tau, \tau][\text{dB}],$$

with which the analytical approximation of the MSE *per frequency* of the SW estimator is given by

$$\text{MSE}_{\text{sw}} = \begin{cases} \varepsilon_{\text{low}}^2, & \text{SNR}_{\text{out}} < -\tau[\text{dB}] \\ \varepsilon_{\text{low}}^2 \cdot f_{\tau} + \varepsilon_{\text{high}}^2 \cdot (1 - f_{\tau}), & |\text{SNR}_{\text{out}}| \leq \tau[\text{dB}] \\ \varepsilon_{\text{high}}^2, & \text{SNR}_{\text{out}} > \tau[\text{dB}] \end{cases}. \quad (39)$$

We emphasize that while the argument  $\text{SNR}_{\text{out}}$  was omitted for brevity from the functions  $\varepsilon_{\text{low}}^2, \varepsilon_{\text{high}}^2$  and  $f_{\tau}$ , they are all functions of  $\text{SNR}_{\text{out}}$ . Moreover, it is easily verified that the MSE (39) is a continuous function of  $\text{SNR}_{\text{out}}$ . In particular,  $f_{\tau}(\text{SNR}_{\text{out}} = -\tau) = 1$  and  $f_{\tau}(\text{SNR}_{\text{out}} = \tau) = 0$ . Finally, based on our experience, a reasonable choice for  $\tau$  is 6[dB].

## VI. SIMULATION RESULTS

In this section we first present empirical results that corroborate our analytical derivations regarding the predicted performance of the proposed SW estimator (16). Then, we

compare our proposed method with four other methods for three different input signals. Within this simulated experiment, we demonstrate that our proposed SW estimator achieves good performance even when the constant noise spectral level is unknown and is estimated from the observed noisy convoluted signal. Finally, we also demonstrate the accuracy of our performance analysis for two cases of non-Gaussian noise, considering both heavy-tailed Laplace and compactly supported uniform distributed time-domain noise.

### A. Predicted MSE Per Frequency of the SW Estimator

We now examine the MSE *per frequency* of the proposed estimator. As can be seen from (32) and (36), the resulting MSE does not depend on the phase of  $X[k]$ , nor of  $H[k]$ . In addition, the MSE (39) is a function of only two quantities:  $|X[k]|^2$  and  $\sigma_{\text{eff}}^2[k] = S_v[k]/|H[k]|^2$ . Thus, in general, a surface plot is sufficient to fully describe the dependence of the MSE on  $|X[k]|$  and  $\sigma_{\text{eff}}^2[k]$ . However, for enhanced visibility we present only two representative slices of this surface. Specifically, Fig. 3 presents the empirical and analytically predicted MSE (39) of the SW estimator, as well as the predicted MSEs of the LS estimator (8) and the MSE of the (unrealizable) optimal solution for reference. While in Fig. 3a  $X[k] = 1$  is fixed and  $\sigma_{\text{eff}}^2[k]$  is varied, in Fig. 3b  $\sigma_{\text{eff}}^2[k] = 1$  and we vary  $X[k]$ . The noise  $V[k]$  was drawn from the circular CN distribution, and each point in the graph is the average of  $10^6$  independent trials.

First, it is evident that the analytically predicted MSE (39) is in excellent fit with the empirical results, verifying that our analytical analysis of the expected performance in terms of MSE is fairly accurate. Second, as explained in Subsection V-A, it can be seen that the MSE of our estimator depends on the unknown signal. In particular, the noise-suppression mechanism is evident in the low SNR regime. This is in stark contrast to the LS estimator, whose MSE (34) is independent of the signal, and is therefore  $\rho[\text{dB}]$  higher than the MSE of the SW estimator at low SNRs. Finally, in compliance with (38), the performance of our estimator is asymptotically optimal as  $\text{SNR}_{\text{out}} \rightarrow \infty$ , similarly to the LS estimator.

Note that we do not assume to have prior knowledge on the unknown signal's DFT structure, thus each frequency component may have any arbitrary SNR. Therefore, a desirable estimator will provide good performance in terms of MSE (preferably) for any output SNR *per frequency*. Figs. 3a and 3b show that our proposed estimate has this property, where the “price” paid for this overall SNR behavior is a local performance degradation in the intermediate SNR region, in which threshold-type estimators generally suffer the most.

### B. Comparison to Other Deconvolution Methods

Consider the following three signals of length  $N = 100$ ,

$$X_1[k] = \left[ \frac{2\pi}{\Delta} \left( \text{rect}\left(\frac{\Omega}{2\pi}\right) * \text{tri}\left(\frac{\Omega}{\Delta}\right) \right) \right] \Big|_{\Omega=6\Delta\omega_k}, \quad (40)$$

$$X_2[k] = \left[ e^{-|\Omega|^2} \right] \Big|_{\Omega=\sqrt{\Delta}\omega_k}, \quad (41)$$

$$X_3[k] = \sum_{\ell=1}^4 (\delta[k-8\ell] + \delta[k+8\ell]), \quad (42)$$

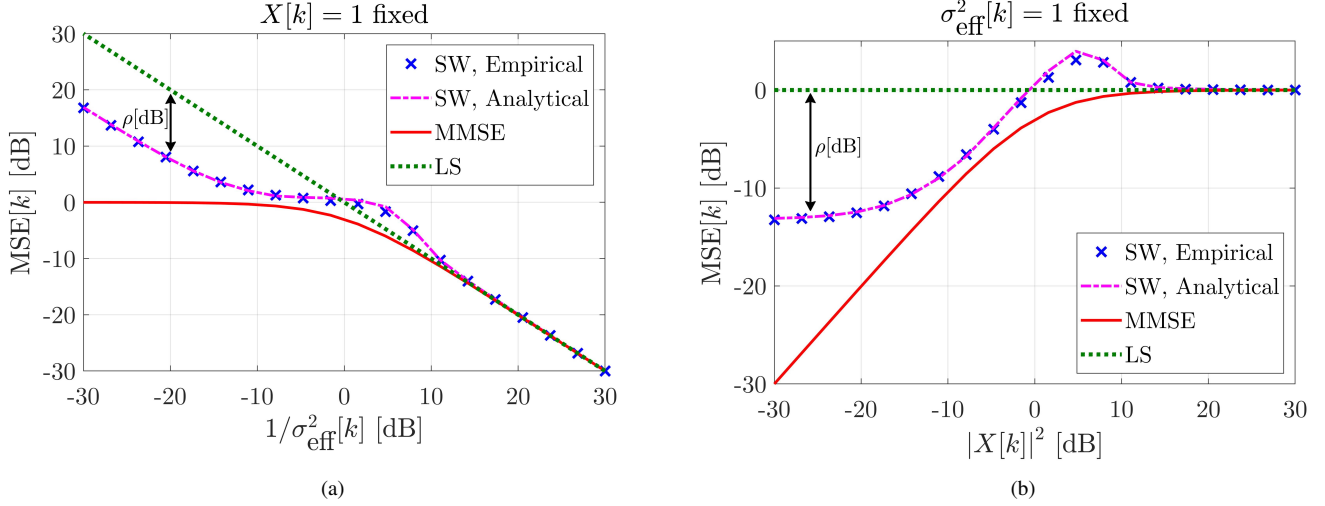


Fig. 3: The MSE of the  $k$ -th frequency component vs. (a) noise power (b) signal power. Here,  $V[k]$  is zero-mean CN, and the empirical results were obtained by averaging  $10^6$  independent trials. A good fit is seen between the analytical prediction and the empirical results. It is seen that in the low SNR regime the SW estimator reduces the MSE in  $\sim 13$  [dB] relative to the LS estimator, while retaining asymptotic optimality in the high SNR regime.

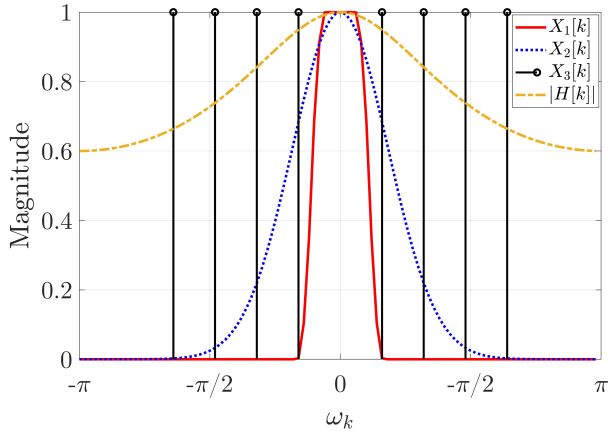


Fig. 4: The DFT magnitudes of the unknown signals  $\{X_i[k]\}_{i=1}^3$  and the known filter  $|H[k]|$  with  $\alpha = 0.25$  for  $N = 100$ .  $X_1[k]$ , bandlimited signal,  $X_2[k]$ , Gaussian pulse,  $X_3[k]$ , narrowband, frequency-domain sparse signal.

with  $\Delta = 1.5$ , and an LTI system with a frequency response

$$H[k] = \frac{1 - \alpha}{1 - \alpha \cdot e^{-j\omega_k}}, \quad \alpha \in (-1, 1), \quad (43)$$

where  $\omega_k \triangleq \frac{2\pi}{N}k$ ,  $*$  denotes continuous convolution,  $\delta[\cdot]$  denotes Kronecker's delta, and  $\text{rect}(\cdot)$ ,  $\text{tri}(\cdot)$  are the standard rectangular and triangular functions, resp. Notice that (40), (41) and (42) are the DFTs of a bandlimited pulse, a Gaussian (approximately bandlimited) pulse, and a narrowband, frequency-domain sparse signal, resp. These functions are thus representative of common physical signals in various applications. Further, the frequency response (43) corresponds to an FIR filter, approximating<sup>1</sup> the infinite impulse response  $h[n] = (1 - \alpha)(-\alpha)^n u[n]$  via truncation, where  $u[n]$  is the Heaviside step function. For negative values of  $\alpha$ ,  $H[k]$  is a non-ideal high pass filter, whereas for positive values,  $H[k]$  is a non-ideal low pass filter. Here, we set  $\alpha = 0.25$ , with which  $H[k]$  has approximately the same effect as the smooth blur

<sup>1</sup>In our case, for  $N = 100$ , the approximation error is completely negligible: for  $\alpha = 0.25$ , already at  $n = 50$  we have  $h[50] \approx -2.3666 \cdot 10^{-30}$ .

considered in [17] (see Subsection 2.1, Fig. 2a therein). For simplicity, we consider the case of white noise, thus the PSD of  $v[n]$  is  $S_v[k] = \sigma_v^2$  for all  $k$ . The magnitudes  $\{|X_i[k]|\}_{i=1}^3$  and  $|H[k]|$  with  $\alpha = 0.25$  are presented in Fig. 4. Observe that with the signals (40)–(42) and the system (43), the values  $\{|X_i[k]H[k]|^2\}$  range from 0 to 1 in (almost) all the range. Thus, by varying  $\sigma_v^2$ , the following empirical evaluation puts to test the considered deconvolution methods below in a very wide range of output SNR *per frequency*—from  $-\infty$  [dB] to  $\sim 40$  [dB]—which fairly covers the output SNR range of practical interest.

We compare the MSE (5) for the signals (40)–(42) and the system (43), achieved by the following five methods:

- i. The naïve LS estimator (also known as inverse filter) (8);
- ii. The grand-mean shrinkage of the Stein unbiased risk estimate type (SURE, [38], Eq. (4.2));
- iii. The Tikhonov (TIK) regularization-based [39],

$$G_{\text{TIK}}[k] \triangleq \frac{H^*[k]}{|H[k]|^2 + \frac{\sigma_v^2}{P_x}}, \quad (44)$$

where  $P_x \triangleq \frac{1}{N} \sum_{k=0}^{N-1} |X[k]|^2 \in \mathbb{R}^+$  is the (known or estimated) average power of the unknown input signal;

- iv. The minimum average MSE Modified Wiener (MW, [27], Eq. (9)),

$$G_{\text{MW}}[k] \triangleq \frac{1}{H[k]} \cdot \frac{1}{1 + q \cdot \frac{1}{\widehat{\text{SNR}}_{\text{out},i}[k]}}, \quad (45)$$

where  $q$  is an adjustable noise-control parameter and  $\widehat{\text{SNR}}_{\text{out},i}[k] \triangleq \max(\widehat{\text{SNR}}_{\text{out}}[k] - 1, 0)$  is an improved output SNR estimator<sup>2</sup> since  $\mathbb{E}[\widehat{\text{SNR}}_{\text{out}}[k]] = \text{SNR}_{\text{out}}[k] + 1$ ;

- v. Our proposed SW estimator (16).

Note that LS and SURE are fully data-driven estimators. Further, note that TIK (44) is the optimal filter (11) for an input signal with a constant DFT, i.e.,  $|X[k]|^2 = P_x$  for all  $k \in \{0, \dots, N-1\}$ . However, for signals with a non-constant

<sup>2</sup>Note that an output SNR estimate is not specified in [27]. Nevertheless, for MW, we use the improved, less biased estimate  $\widehat{\text{SNR}}_{\text{out},i}[k]$ .

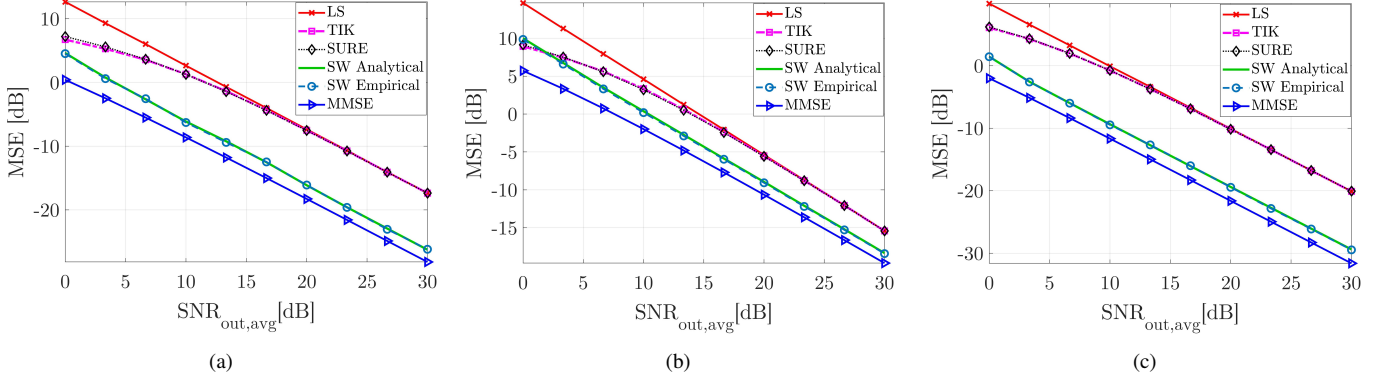


Fig. 5: MSE vs. the *average* output SNR. As seen, our estimator exhibits the best overall performance, and is the closest to the unrealizable optimal solution. Results were obtained by  $10^3$  independent trials for  $N = 100$ . (a)  $X_1[k]$ , bandlimited signal (b)  $X_2[k]$ , Gaussian pulse (c)  $X_3[k]$ , Narrowband signal.

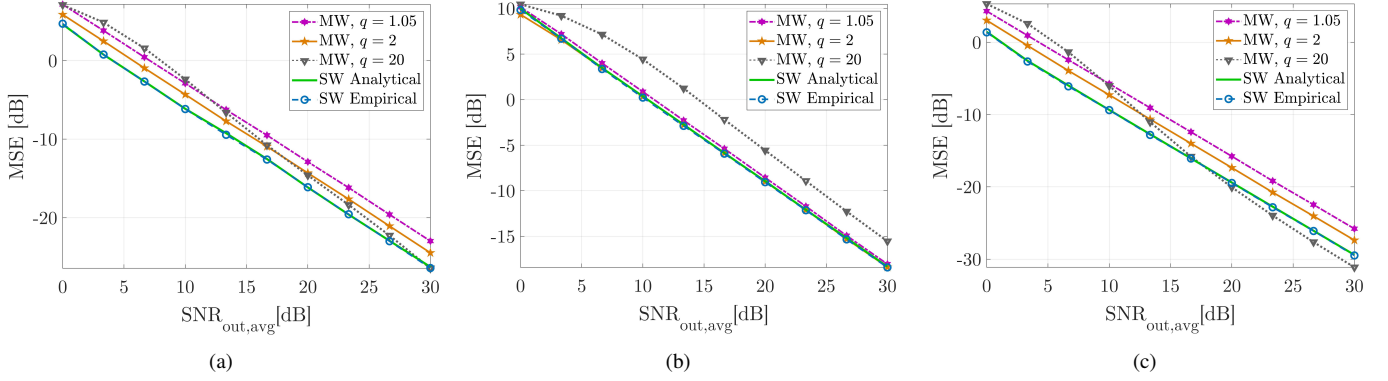


Fig. 6: MSE vs. the *average* output SNR. While the MW estimator requires careful calibration of the tuning parameter  $q$ , and its performance are quite sensitive w.r.t.  $q$ , the proposed SW estimator requires no tuning and provides better performance overall. Results were obtained by  $10^3$  independent trials for  $N = 100$ . (a)  $X_1[k]$ , bandlimited signal (b)  $X_2[k]$ , Gaussian pulse (c)  $X_3[k]$ , Narrowband signal.

DFT, in practice, since  $P_x$  is unknown, the regularization constant ( $\sigma_v^2/P_x$ ), sometimes termed the “Tikhonov parameter”, has to be tuned *ad-hoc*. Specifically, in our simulations we consider an ideal (or “oracle”) TIK estimate, which enjoys the advantage of available side information—the exact power of the unknown input signal  $x[n]$ . As for MW (45), since its performance is highly sensitive to the particular choice of the tuning parameter  $q$ , a more detailed comparison for a few values of  $q$ , along with a short discussion, will be shortly provided separately. Finally, as a benchmark for the best attainable performance in terms of MMSE, we add to our simulations  $\hat{X}_{\text{opt}}[k]$  of (11). This estimator is of course unrealizable, however it is still the optimal MMSE deconvolution-type (3) solution. The following results were obtained by averaging  $10^3$  independent trials.

Fig. 5 presents the MSE (5) vs. the *average* output SNR over all the output SNRs *per frequency*, defined as

$$\text{SNR}_{\text{out,avg}} \triangleq \frac{1}{N} \sum_{k=0}^{N-1} \text{SNR}_{\text{out}}[k].$$

Evidently, our proposed estimator gives a considerable improvement in the resulting MSE relative to the LS, TIK and SURE estimators, reaching a gain of almost an order of magnitude (up to  $\sim 9$  dB). Moreover, it is seen from Figs. 5a and 5c that our proposed estimator offers a more significant enhancement relative to these non-threshold-type methods for the bandlimited and sparse frequency-domain signals. In

addition, although at the low SNR regime it is slightly inferior, our estimator is also superior to the other methods even for a non-sparse, only approximately bandlimited signal (41) for a sufficiently high *average* output SNR (in this example from  $\sim 2$  dB), as evident from Fig. 5b.

Next, we compare our proposed estimator with MW (45), which depends on the tuning parameter  $q$ . Note that  $q$  is fixed w.r.t. the different frequencies (i.e., the index  $k$ ). Thus, we evaluate its performance for  $q = 1.05, 2, 20$ , so as to examine different trade-offs between “the mean-squared estimation error and the mean-squared filtered noise” (see [27], Eq. (4)), referred here as MSE and noise suppression, resp.:

- With  $q = 1.05$ , the MW tends to naively mimic the optimal solution (11) ( $\sim 5\%$  noise suppression weight);
- With  $q = 2$ , equal weights are given to MSE minimization and noise suppression; and
- With  $q = 20$ , noise suppression is preferred over accurate signal reconstruction ( $\sim 95\%$  noise suppression weight).

Indeed, for many possible signals in various applications, while at some frequencies the SNR is very low or even zero, at others it may be very high, thus both noise suppression and MSE minimization are desired. As seen from Fig. 6, relative to the MW with  $q = 1.05$  and  $q = 2$ , corresponding to an approximate naïve imitation of the optimal solution (11) and equal weighting, resp., the SW estimator is uniformly superior for  $X_1$  and  $X_3$ , and performs approximately equality well for  $X_2$ . Further, the local superiority of the MW with  $q = 20$ ,

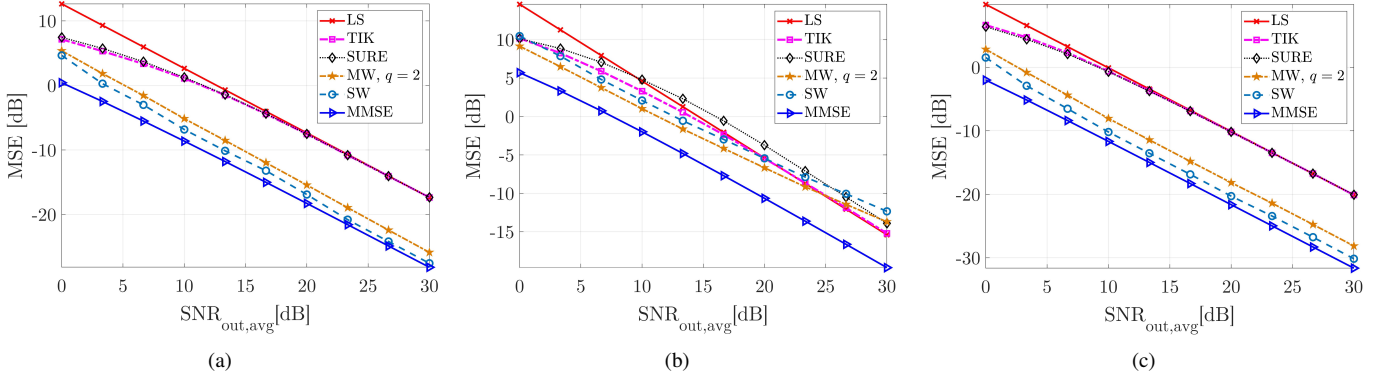


Fig. 7: MSE vs. the *average* output SNR, where the noise variance  $\sigma_v^2$  is unknown, and its estimate  $\hat{\sigma}_v^2$  is used instead. Results were obtained by averaging  $10^3$  independent trials. (a)  $X_1[k]$ , bandlimited signal (b)  $X_2[k]$ , Gaussian pulse (c)  $X_3[k]$ , Narrowband signal. It is seen that our estimator exhibits the best performance for  $X_1$  and  $X_3$ , whereas for  $X_2$ , different estimators dominate all the others in different SNR regions.

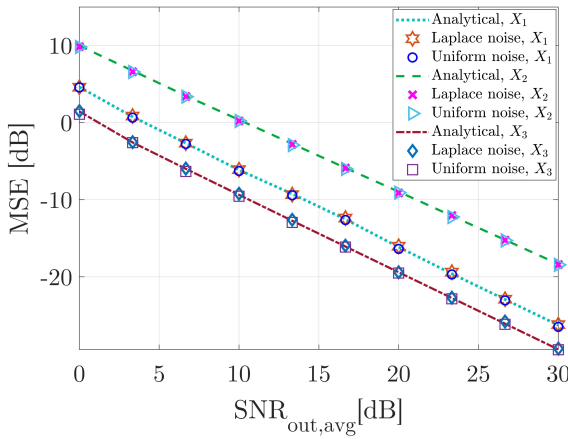


Fig. 8: MSE of the SW estimator vs. the average output SNR for the signals  $X_1, X_2$  and  $X_3$  and non-Gaussian noise. Evidently, the CN distribution assumption for the noise *pre frequency*  $V[k]$  enables to accurately assess the predicted MSE. Results were obtained by averaging  $10^3$  independent trials.

corresponding to noise suppression oriented weighting, for  $X_3$  at the high SNR regime *only*, is at the cost of greater degradation in the low SNR regime, and uniform inferiority to the SW estimator for  $X_1$  and  $X_2$ . It is important to bear in mind that, in practice, since the input signal is unknown, and therefore the *per frequency* SNRs are unknown as well, the MSE cannot be evaluated, hence it is not clear how one chooses<sup>3</sup> the tuning parameter  $q$ , which clearly affects the resulting performance considerably. In contrast, since our proposed SW estimator is free of such a tuning parameter, in some sense, it implicitly chooses the proper “weighting”, according to the *per frequency* estimated output SNR (22).

Unlike the previous comparison to LS, TIK and SURE in Fig. 5, which emphasized the performance gain in terms of MSE, this comparison to MW emphasizes the inherent *adaptivity* property of our proposed solution. Accordingly, as also seen from Fig. 6, none of the three different MW estimators perform better than our proposed solution for all three signals. Instead, the SW estimator is the most stable, and exhibits the best overall performance, considering different signals with different average output SNRs.

<sup>3</sup>[27] does not provide a method for choosing the tuning parameter  $q$ , but rather only discusses the effects of choosing different values of  $q$ .

Next, we compare the methods under a setting where the noise level  $\sigma_v^2$  is unknown and has to be estimated. Following Donoho *et al.* [35] (Subsection 6.1.1.), we use the Median Absolute Deviation (MAD) [40] to estimate  $\sigma_v$ ,

$$\hat{\sigma}_v \triangleq \frac{1}{\sqrt{2}} \cdot 1.4826 \cdot [\text{MAD}(\Re\{Y\}) + \text{MAD}(\Im\{Y\})]. \quad (46)$$

Here  $Y \triangleq [Y[0] \dots Y[N-1]]^T \in \mathbb{C}^{N \times 1}$ , and as discussed in [35], (46) is accurate when the input signal is approximately sparse in the frequency domain. Accordingly,  $\hat{\sigma}_v^2$  replaces  $\sigma_v^2$  for all methods. In particular, we have  $\hat{Z}[k] = Y[k]/\hat{\sigma}_v^2$  instead of  $Z[k]$  for the SW estimator, and for a fair comparison, TIK now uses the estimated signal power

$$\hat{P}_x \triangleq \frac{1}{N} \sum_{k=0}^{N-1} |Y[k]|^2 - \hat{\sigma}_v^2 \triangleq \hat{P}_y - \hat{\sigma}_v^2,$$

rather than the true  $P_x$ . For MW, we choose  $q = 2$ , which is the most stable for the signals under consideration. The LS estimator simply applies the inverse filter and does not use  $\sigma_v^2$ . Thus, its performance in this setting is exactly the same as in the previous setting, where  $\sigma_v^2$  is known (Fig. 5). Nevertheless, we present it here as well for a convenient comparison with all the other methods under consideration.

Note that in our setting, where no assumptions on the input signal’s DFT  $X[k]$  are made, (46) is generally biased and overestimated. Therefore, the estimated output SNR (22) will now be lower. In turn, this will cause performance degradation at frequencies with high and intermediate SNR, since a higher shrinkage value (20) will be wrongfully used. However, at frequencies with low SNR, the noise “defense mechanism” discussed in Subsection V-A will be intensified, and will result in performance enhancement. Thus, the overall deviation in the MSE (5) depends on the true, *unknown* output SNR distribution over all frequencies. For example, bandlimited and/or sparse frequency-domain signals, whose majority of frequencies have low output SNR, are expected to have enhanced, or at least not degraded, overall MSE performance.

Fig. 7 shows the MSE (5) vs. the *average* output SNR when  $\hat{\sigma}_v^2$  replaces  $\sigma_v^2$ . As seen, our estimator exhibits the best performance for  $X_1$  and  $X_3$ , the bandlimited and sparse signals, resp. Further, a slight improvement up to  $\sim 1$ [dB] w.r.t.



the previous setting is also observed, as expected, due to over-estimation of  $\sigma_v^2$ . For  $X_2$ , which is not sparse or bandlimited, our proposed estimator exhibits performance degradation of up to  $\sim 6$ [dB] w.r.t. the previous setting in which  $\sigma_v^2$  is known. Yet, it is still competitive, as different estimators dominate in different *average* output SNR regions. Therefore, our proposed method provides reliable deconvolution even when the noise variance is unknown.

Finally, we present in Fig. 8 the analytically predicted (39) and empirical MSEs of the SW estimator for the signals (40)–(42), however now for time-domain measurements  $y[n]$  contaminated either by Laplace or by uniform distributed noise  $v[n]$ . As expected, an excellent fit is evident—due to the DFT (4), and by virtue of the CLT, the frequency-domain noise  $V[k]$  is approximately distributed as CN. This is in compliance with our assumption on the noise’s CN distribution *per frequency* in Section V.

## VII. CONCLUSION

In the framework of deterministic signals reconstruction, we presented a non-iterative, fully data-driven robust deconvolution method, which is based on mild assumptions regarding the unknown signal. Furthermore, our method, termed “Self-Wiener” filtering, is free of any tuning parameters, and is inherently particularly suitable for bandlimited or frequency-domain sparse signals. We provided an analytical performance analysis of the proposed estimator, which enables to accurately assess its predicted performance, and thus to better characterize its strengths and weaknesses. The performance gain over other common (not necessarily) data-driven alternatives was presented in simulations, reaching up to almost an order of magnitude reduction in the residual MSE relative to these methods.

## APPENDIX A PROOF OF THEOREM 3

To show that in the low SNR regime the MSE (26) can be approximated by the expression (32), we expand the quantities (29), (27) and (28) at  $|\eta| \ll 1$ . Starting with (29), we have by definition

$$p = \Pr(|Z| > 2) = e^{-|\eta|^2} \int_{2\sqrt{2}}^{\infty} x e^{-\frac{x^2}{2}} I_0(\sqrt{2}|\eta|x) dx, \quad (47)$$

where  $I_0$  is the modified Bessel function of the first kind. Since  $p$  is analytic in  $|\eta|$ , performing a Taylor expansion of (47) and using known results regarding the Bessel function yields

$$p = \int_{2\sqrt{2}}^{\infty} x e^{-\frac{x^2}{2}} dx + \mathcal{O}(|\eta|^2) = e^{-4} + \mathcal{O}(|\eta|^2). \quad (48)$$

Next, we turn to (27), and write it as

$$\mathbb{E} \left[ \widehat{X}_{\text{sw}} \middle| |Z| > 2 \right] \triangleq g_1(\eta) = g_1(0) + \mathcal{O}(|\eta|).$$

Recall that  $Z|_{\eta=0} = \widetilde{V}$ , thus

$$g_1(0) = \frac{\sqrt{S_v}}{H} \mathbb{E} \left[ \frac{2(\widetilde{V}^*)^{-1}}{1 - \sqrt{1 - 4|\widetilde{V}|^{-2}}} \middle| |\widetilde{V}| > 2 \right].$$

Since  $\widetilde{V} \sim \mathcal{CN}(0, 1)$ , it is invariant to rotations. As the domain  $|\widetilde{V}| > 2$  is also circularly symmetric, it follows that  $g_1(0) = 0$ . Hence,

$$\mathbb{E} \left[ \widehat{X}_{\text{sw}} \middle| |Z| > 2 \right] = \mathcal{O}(|\eta|). \quad (49)$$

Similarly, we write (28) as

$$\mathbb{E} \left[ \left| \widehat{X}_{\text{sw}} \right|^2 \middle| |Z| > 2 \right] \triangleq g_2(\eta) = g_2(0) + \mathcal{O}(|\eta|). \quad (50)$$

Using (20), (13) and the relation  $\widehat{X}_{\text{ls}} = \frac{\sqrt{S_v}}{H} Z$ , we have

$$\begin{aligned} g_2(0) &= \mathbb{E} \left[ \left| \widehat{X}_{\text{sw}} \right|^2 \middle| |\widetilde{V}| > 2 \right] = \\ &= \frac{S_v}{4|H|^2} \cdot \mathbb{E} \left[ \left| \widetilde{V} \right|^2 \left( 1 + \sqrt{1 - 4|\widetilde{V}|^{-2}} \right)^2 \middle| |\widetilde{V}| > 2 \right] = \\ &= \frac{\sigma_{\text{eff}}^2}{2} \cdot \mathbb{E} \left[ \left| \widetilde{V} \right|^2 + \sqrt{|\widetilde{V}|^4 - 4|\widetilde{V}|^2} - 2 \middle| |\widetilde{V}| > 2 \right]. \end{aligned}$$

Here,  $|\widetilde{V}|^2 \triangleq \xi^2/2$ , where  $\xi^2$  follows a chi-square distribution with two degrees of freedom. Its density is simply an exponential with rate  $1/2$ , namely  $f(t) = \frac{1}{2} \exp(-t/2)$ . Furthermore, the domain of integration is  $\xi^2 > 8$ , and as we showed in (48),  $p|_{\eta=0} = \Pr(|Z| > 2)|_{\eta=0} = \Pr(\xi^2 > 8) = e^{-4}$ . Hence,

$$\begin{aligned} &\frac{\sigma_{\text{eff}}^2}{2} \cdot \mathbb{E} \left[ \left| \widetilde{V} \right|^2 + \sqrt{|\widetilde{V}|^4 - 4|\widetilde{V}|^2} - 2 \middle| |\widetilde{V}| > 2 \right] = \\ &\frac{\sigma_{\text{eff}}^2}{2} \cdot \frac{1}{p|_{\eta=0}} \cdot \int_8^{\infty} \left[ \frac{t}{2} + \sqrt{\frac{t^2}{4} - 2t} - 2 \right] \frac{1}{2} e^{-\frac{t}{2}} dt = \sigma_{\text{eff}}^2 \cdot \frac{\rho}{e^{-4}}, \end{aligned}$$

where the scalar  $\rho$  is given by

$$\begin{aligned} \rho &= \frac{1}{2} \int_8^{\infty} \left[ \frac{t}{2} + \sqrt{\frac{t^2}{4} - 2t} - 2 \right] \frac{1}{2} e^{-\frac{t}{2}} dt \\ &= \frac{1}{2} [5e^{-4} + 2e^{-2}K_1(2) - 2e^{-4}] \approx 0.0464, \end{aligned} \quad (51)$$

and  $K_1$  is the modified Bessel function of the second kind. We thus conclude that  $g_2(0) = \sigma_{\text{eff}}^2 \cdot \rho \cdot e^4$ . Therefore, (50) reads

$$\mathbb{E} \left[ \left| \widehat{X}_{\text{sw}} \right|^2 \middle| |Z| > 2 \right] = \frac{\sigma_{\text{eff}}^2 \cdot \rho}{e^{-4}} + \mathcal{O}(|\eta|). \quad (52)$$

Finally, substituting (48), (49) and (52) into (26) gives (32), as required.  $\blacksquare$

## APPENDIX B PROOF OF THEOREM 4

To prove the theorem, we shall use the following lemma.

*Lemma 1:* Let  $Z = \eta + \widetilde{V}$ , where  $\widetilde{V} \sim \mathcal{CN}(0, 1)$ . Then, as  $|\eta| \rightarrow \infty$ ,

$$\mathbb{E} \left[ \frac{1}{|Z|^2} \middle| |Z| > 2 \right] = \frac{1}{|\eta|^2} + \mathcal{O} \left( \frac{1}{|\eta|^4} \right), \quad (53)$$

$$\mathbb{E} \left[ \frac{\widetilde{V}}{|\eta||Z|^2} \middle| |Z| > 2 \right] = \mathcal{O} \left( \frac{1}{|\eta|^4} \right). \quad (54)$$

*Proof of Lemma 1:* Let us write

$$\frac{1}{|Z|^2} = \frac{1}{|\eta + \tilde{V}|^2} = \frac{1}{|\eta|^2} \cdot \frac{1}{1 + 2\Re\{\tilde{V}/\eta\} + |\tilde{V}|^2/|\eta|^2}.$$

As  $|\eta| \rightarrow \infty$ , with high probability, up to exponentially small terms in  $|\eta|$ ,  $|\tilde{V}/\eta| \ll 1$ . Under this event, we may thus perform a Taylor expansion  $\frac{1}{1-x} = \sum_{n=0}^{\infty} x^n$  to obtain

$$\frac{1}{|Z|^2} = \frac{1}{|\eta|^2} \cdot \left(1 - 2\Re\{\tilde{V}/\eta\}\right) + \mathcal{O}_P\left(\frac{1}{|\eta|^4}\right). \quad (55)$$

We now take the conditional expectation. However, since  $|\eta| \gg 1$ , we may neglect the condition  $|Z| > 2$ , and perform the integration over all of the domain of  $\tilde{V}$ . This introduces a negligible error, exponentially small in  $|\eta|$ . Since  $\mathbb{E}[\tilde{V}] = 0$ , taking the expectation of (55) gives (53).

To prove (54), we again use (55) to have

$$\frac{\tilde{V}}{\eta|Z|^2} = \frac{1}{|\eta|^2} \cdot \left(\frac{\tilde{V}}{\eta} - 2\frac{\tilde{V}}{\eta}\Re\left\{\frac{\tilde{V}}{\eta}\right\}\right) + \mathcal{O}_P\left(\frac{1}{|\eta|^4}\right). \quad (56)$$

We now take the expectation in the same way as above, namely neglect the condition  $|Z| > 2$  and integrate over all of the domain of  $\tilde{V}$ , thus introducing an error exponentially small in  $|\eta|$ . Since

$$\mathbb{E}\left[\left(\tilde{V}/\eta\right)\Re\left\{\tilde{V}/\eta\right\}\right] = \frac{1}{2} \cdot \mathbb{E}\left[|\tilde{V}/\eta|^2\right] = \frac{1}{2|\eta|^2},$$

taking the expectation of (56) gives (54).  $\blacksquare$

*Proof of Theorem 4:* Note that for  $|\eta| \gg 1$ , with high probability (up to deviations exponentially small in  $|\eta|$ ),  $|Z| = |\eta + \tilde{V}| \gg 1$ . Hence, using the Taylor expansion  $\sqrt{1-\epsilon} = 1 - \frac{\epsilon}{2} + \mathcal{O}(\epsilon^2)$  in (20) gives

$$\hat{X}_{\text{sw}} = \left(X + \frac{\sqrt{S_v}}{H}\tilde{V}\right) \cdot (1 - |Z|^{-2} + \mathcal{O}_P(|\eta|^{-4})). \quad (57)$$

Let us start with (27). Using (57), we have that

$$\mathbb{E}\left[\hat{X}_{\text{sw}} \mid |Z| > 2\right] = X \cdot \mathbb{E}\left[1 - |Z|^{-2} + \mathcal{O}_P(|\eta|^{-4}) \mid |Z| > 2\right] + \quad (58)$$

$$\frac{\sqrt{S_v}}{H} \cdot \mathbb{E}\left[\tilde{V}(1 - |Z|^{-2} + \mathcal{O}_P(|\eta|^{-4})) \mid |Z| > 2\right]. \quad (59)$$

Regarding the term (58), using (53) of Lemma 1,

$$\begin{aligned} X \cdot \mathbb{E}\left[1 - |Z|^{-2} + \mathcal{O}_P(|\eta|^{-4}) \mid |Z| > 2\right] &= \\ X \cdot \left(1 - \frac{1}{|\eta|^2} + \mathcal{O}\left(\frac{1}{|\eta|^4}\right)\right). \end{aligned}$$

As for (59), up to exponentially small terms in  $|\eta|$ ,  $\mathbb{E}[\tilde{V} \mid |Z| > 2] = 0$ . Therefore, using (54) of Lemma 1,

$$\begin{aligned} \frac{\sqrt{S_v}}{H} \cdot \mathbb{E}\left[\tilde{V}(1 - |Z|^{-2} + \mathcal{O}_P(|\eta|^{-4})) \mid |Z| > 2\right] &= \\ X \cdot \left(\mathbb{E}\left[\frac{\tilde{V}}{\eta|Z|^2} \mid |Z| > 2\right] + \mathcal{O}\left(\frac{1}{|\eta|^4}\right)\right) &= X \cdot \mathcal{O}\left(\frac{1}{|\eta|^4}\right) \end{aligned}$$

Hence, the above gives

$$\mathbb{E}\left[\hat{X}_{\text{sw}} \mid |Z| > 2\right] = X \cdot \left(1 - \frac{1}{|\eta|^2} + \mathcal{O}\left(\frac{1}{|\eta|^4}\right)\right). \quad (60)$$

Next, we turn to analyze (28). Note that

$$\left[1 - |Z|^{-2} + \mathcal{O}_P(|\eta|^{-4})\right]^2 = 1 - 2|Z|^{-2} + \mathcal{O}_P(|\eta|^{-4}).$$

Thus, using the relation  $|\hat{X}_{\text{ls}}|^2 = \sigma_{\text{eff}}^2 \cdot |Z|^2 = \frac{|X|^2}{|\eta|^2} \cdot |Z|^2$ ,

$$\begin{aligned} |\hat{X}_{\text{sw}}|^2 &= \frac{|X|^2}{|\eta|^2} \cdot |Z|^2 \cdot \left(1 - 2|Z|^{-2} + \mathcal{O}_P(|\eta|^{-4})\right) \\ &= |X|^2 \cdot \left(\frac{|Z|^2}{|\eta|^2} - \frac{2}{|\eta|^2} + \mathcal{O}_P(|\eta|^{-4})\right). \end{aligned}$$

Using  $\mathbb{E}[|Z|^2] = |\eta|^2 + 1$  and similar arguments as before yield that

$$\mathbb{E}\left[|\hat{X}_{\text{sw}}|^2 \mid |Z| > 2\right] = |X|^2 \cdot \left(1 - \frac{1}{|\eta|^2} + \mathcal{O}\left(\frac{1}{|\eta|^4}\right)\right). \quad (61)$$

Since  $|X|^2/|\eta|^4 = \sigma_{\text{eff}}^2/\text{SNR}_{\text{out}}$ , substituting (60) and (61) into (26) gives (36).  $\blacksquare$

## APPENDIX C

### MSE ANALYSIS OF REAL-VALUED DFT COMPONENTS

The analysis for the real-valued DFT bins, corresponding to the indices  $k = 0, N/2$ , is very similar to the analysis presented in Section V and above. In these cases  $\tilde{V} \sim \mathcal{N}(0, 1)$ , thus the probability  $p[k]$  reads

$$k = 0, \frac{N}{2} : p[k] = \Pr(|Z[k]| > 2) = Q(2 - \eta[k]) + Q(2 + \eta[k]), \quad (62)$$

where  $Q(\cdot)$  is the Q-function:  $Q(x) \triangleq \frac{1}{2\pi} \int_x^\infty e^{-0.5t^2} dt$  (recall that  $\eta[k]$  is real-valued for  $k = 0, N/2$ ).

For the low SNR approximation, it is easy to verify that,

$$|\eta| \ll 1 : p = 2Q(2) + \mathcal{O}(|\eta|), \quad (63)$$

and that (27) is still

$$\mathbb{E}\left[\hat{X}_{\text{sw}} \mid |Z| > 2\right] = \mathcal{O}(|\eta|),$$

from symmetry considerations. However, (28) now reads

$$\mathbb{E}\left[|\hat{X}_{\text{sw}}|^2 \mid |Z| > 2\right] = \frac{|X|^2 \varrho}{2Q(2)|\eta|^2} + \mathcal{O}(|\eta|), \quad (64)$$

where

$$\begin{aligned} \varrho &\triangleq \int_2^\infty \left[v^2 - 2 + \sqrt{v^4 - 4v^2}\right] \frac{1}{\sqrt{2\pi}} e^{-\frac{v^2}{2}} dv \\ &= \frac{e^{-2}}{2} + e^{-2} \sqrt{\frac{2}{\pi}} - Q(2) \approx 0.1529, \end{aligned}$$

an order of magnitude greater than  $\rho$  in (51) of the complex-valued case. Using the updated terms (63) and (64), the MSE (26) at frequencies with low SNR, namely  $|\eta| \ll 1$ , for the real-valued DFT components is given by

$$\begin{aligned} \text{MSE}_{\text{sw}} &= |X|^2 + \varrho \cdot \sigma_{\text{eff}}^2 + \mathcal{O}(|\eta|) \\ &= |X|^2 \cdot \left(1 + \frac{\varrho}{\text{SNR}_{\text{out}}}\right) + \mathcal{O}(\sqrt{\text{SNR}_{\text{out}}}), \end{aligned}$$

so the MSE is greater for the real-valued DFT components.

The high SNR approximation is also obtained in the same fashion, only now  $Z \sim \mathcal{N}(\eta, 1)$ . It follows that for  $|\eta| \gg$

1, (53) and (54) from Lemma 1 hold in this case as well. Accordingly, using the fact that  $\mathbb{E}[Z^2] = \eta^2 + 1$  and similar arguments as in Theorem 4, it is easy to verify that (60) and (61) hold true when  $Z$  is normal, rather than CN. Therefore, the MSE (26) at frequencies with high SNR, namely  $|\eta| \gg 1$ , for the *real-valued* DFT components is given by

$$\begin{aligned} \text{MSE}_{\text{sw}} &= (1 - p) \cdot |X|^2 + p \cdot \frac{|X|^2}{|\eta|^2} + \mathcal{O}\left(\frac{|X|^2}{|\eta|^4}\right) \\ &= (1 - p) \cdot |X|^2 + p \cdot \sigma_{\text{eff}}^2 + \mathcal{O}\left(\frac{\sigma_{\text{eff}}^2}{\text{SNR}_{\text{out}}}\right), \end{aligned}$$

with  $p = Q(2 - \sqrt{\text{SNR}_{\text{out}}}) + Q(2 + \sqrt{\text{SNR}_{\text{out}}})$  as in (62).

## REFERENCES

- [1] S. M. Riad, "The Deconvolution Problem: An Overview," *Proc. of the IEEE*, vol. 74, no. 1, pp. 82–85, 1986.
- [2] J. M. Mendel, *Maximum-Likelihood Deconvolution: A Journey into Model-Based Signal Processing*. Springer Science & Business Media, 2012.
- [3] F. C. C. De Castro, M. C. F. De Castro, and D. S. Arantes, "Concurrent Blind Deconvolution for Channel Equalization," in *ICC 2001. IEEE International Conference on Communications. Conference Record (Cat. No. 01CH37240)*, vol. 2, 2001, pp. 366–371.
- [4] L. Ljung, "System Identification," *Wiley Encyclopedia of Electrical and Electronics Engineering*, pp. 1–19, 1999.
- [5] Y. Tendo and J.-M. Morel, "An Optimal Blind Temporal Motion Blur Deconvolution Filter," *IEEE Signal Processing Letters*, vol. 20, no. 5, pp. 523–526, 2013.
- [6] D. Krishnan and R. Fergus, "Fast Image Deconvolution Using Hyper-Laplacian Priors," in *Advances in neural information processing systems*, 2009, pp. 1033–1041.
- [7] S. Subramaniam, A. P. Petropulu, and C. Wendt, "Cepstrum-Based Deconvolution for Speech Dereverberation," *IEEE Trans. Speech Audio Process.*, vol. 4, no. 5, pp. 392–396, 1996.
- [8] C. Schmelzbach and E. Huber, "Efficient Deconvolution of Ground-Penetrating Radar Data," *IEEE Trans. Geosci. Remote Sens.*, vol. 53, no. 9, pp. 5209–5217, 2015.
- [9] J. Wu, J. Van Aardt, and G. P. Asner, "A Comparison of Signal Deconvolution Algorithms Based On Small-Footprint LiDAR Waveform Simulation," *IEEE Trans. Geosci. Remote Sens.*, vol. 49, no. 6, pp. 2402–2414, 2011.
- [10] N. Wiener, *Extrapolation, interpolation, and smoothing of stationary time series*. The MIT press, 1964.
- [11] H. L. Van Trees and K. L. Bell, *Detection Estimation and Modulation Theory*. Wiley, 2013.
- [12] A. Berkhout, "Least-Squares Inverse Filtering and Wavelet Deconvolution," *Geophysics*, vol. 42, no. 7, pp. 1369–1383, 1977.
- [13] Y. C. Eldar, "Robust Deconvolution of Deterministic and Random Signals," *IEEE Trans. Inf. Theory*, vol. 51, no. 8, pp. 2921–2929, 2005.
- [14] L. B. Lucy, "An iterative technique for the rectification of observed distributions," *The astronomical journal*, vol. 79, p. 745, 1974.
- [15] V. M. Patel, G. R. Easley, and D. M. Healy, "Shearlet-Based Deconvolution," *IEEE Trans. Image Process.*, vol. 18, no. 12, pp. 2673–2685, 2009.
- [16] R. Benhaddou, "Deconvolution Model With Fractional Gaussian Noise: A Minimax Study," *Statistics & Probability Letters*, vol. 117, pp. 201–208, 2016.
- [17] I. M. Johnstone, G. Kerkycharian, D. Picard, and M. Raimondo, "Wavelet deconvolution in a periodic setting," *Journal of the Royal Statistical Society: Series B (Statistical Methodology)*, vol. 66, no. 3, pp. 547–573, 2004.
- [18] L. Cavalier and M. Raimondo, "Wavelet Deconvolution With Noisy Eigenvalues," *IEEE Trans. Signal Process.*, vol. 55, no. 6, pp. 2414–2424, 2007.
- [19] A. Bennis and S. M. Riad, "An Optimization Technique for Iterative Frequency-Domain Deconvolution," *IEEE Trans. Instrum. Meas.*, vol. 39, no. 2, pp. 358–362, 1990.
- [20] T. Dhaene, L. Martens, and D. De Zutter, "Extended Bennis-Riad Criterion for Iterative Frequency-Domain Deconvolution," *IEEE Trans. Instrum. Meas.*, vol. 43, no. 2, pp. 176–180, 1994.
- [21] M. Pruksch and F. Fleischmann, "Positive Iterative Deconvolution in Comparison to Richardson-Lucy Like Algorithms," in *Astronomical Data Analysis Software and Systems VII*, vol. 145, 1998, p. 496.
- [22] P. Neveux, E. Sekko, and G. Thomas, "A constrained iterative deconvolution technique with an optimal filtering: Application to a hydrocarbon concentration sensor," *IEEE Trans. Instrum. Meas.*, vol. 49, no. 4, pp. 852–856, 2000.
- [23] M. Welk and M. Erler, "Algorithmic Optimisations for Iterative Deconvolution Methods," In: J. Piater, A. Rodríguez-Sánchez, eds., *Proc. of the 37th Annual Workshop of the Austrian Association for Pattern Recognition (AGM/AAPR)*, vol. 1304.1876, arXiv:1304.7211 [cs.CV], 2013.
- [24] T. B. Bakó and T. Dabóczy, "Improved-Speed Parameter Tuning of Deconvolution Algorithm," *IEEE Trans. Instrum. Meas.*, vol. 65, no. 7, pp. 1568–1576, 2016.
- [25] J. Kalifa and S. Mallat, "Thresholding estimators for linear inverse problems and deconvolutions," *The Annals of Statistics*, vol. 31, no. 1, pp. 58–109, 2003.
- [26] Stoica, Petre and Moses, Randolph L., "Spectral Analysis of Signals," 2005.
- [27] A. Walden, "Robust Deconvolution by Modified Wiener Filtering," *Geophysics*, vol. 53, no. 2, pp. 186–191, 1988.
- [28] K. J. Åström and P. Eykhoff, "System Identification—A Survey," *Automatica*, vol. 7, no. 2, pp. 123–162, 1971.
- [29] A. V. Oppenheim and R. W. Schaffer, *Discrete-Time Signal Processing*, 3rd ed. USA: Prentice Hall Press, 2009.
- [30] R. M. Gray, "Toeplitz and Circulant Matrices: A review," *Foundations and Trends® in Communications and Information Theory*, vol. 2, no. 3, pp. 155–239, 2006.
- [31] P. Holmes and E. T. Shea-Brown, "Stability," *Scholarpedia*, vol. 1, no. 10, p. 1838, 2006, revision #137538.
- [32] D. L. Donoho and I. M. Johnstone, "Adapting to Unknown Smoothness via Wavelet Shrinkage," *Journal of the american statistical association*, vol. 90, no. 432, pp. 1200–1224, 1995.
- [33] J. A. Tropp, J. N. Laska, M. F. Duarte, J. K. Romberg, and R. G. Baraniuk, "Beyond Nyquist: Efficient Sampling of Sparse Bandlimited Signals," *IEEE Trans. Inf. Theory*, vol. 56, no. 1, pp. 520–544, 2009.
- [34] S. Dikmese, Z. Ilyas, P. C. Sofotasios, M. Renfors, and M. Valkama, "Sparse Frequency Domain Spectrum Sensing and Sharing Based on Cyclic Prefix Autocorrelation," *IEEE Journal on Selected Areas in Communications*, vol. 35, no. 1, pp. 159–172, 2016.
- [35] D. L. Donoho, I. M. Johnstone, G. Kerkycharian, and D. Picard, "Wavelet Shrinkage: Asymptopia?" *Journal of the Royal Statistical Society: Series B (Methodological)*, vol. 57, no. 2, pp. 301–337, 1995.
- [36] S. M. Ross, *A First Course in Probability*. Pearson Prentice Hall Upper Saddle River, NJ, 2006, vol. 7.
- [37] A. H. Nuttall, "Some Integrals Involving the  $Q_M$  Function (Corresp.)," *IEEE Trans. on Inf. Theory*, vol. 21, no. 1, pp. 95–96, 1975.
- [38] X. Xie, S. Kou, and L. D. Brown, "SURE Estimates For a Heteroscedastic Hierarchical Model," *Journal of the American Statistical Association*, vol. 107, no. 500, pp. 1465–1479, 2012.
- [39] A. N. Tikhonov and V. Y. Arsenin, "Solutions of ill-posed problems," *New York*, pp. 1–30, 1977.
- [40] C. Leys, C. Ley, O. Klein, P. Bernard, and L. Licata, "Detecting outliers: Do not use standard deviation around the mean, use absolute deviation around the median," *Journal of Experimental Social Psychology*, vol. 49, no. 4, pp. 764–766, 2013.